All-optical Flip-flop based on SMZ with A Feedback-Loop and Multiple Forward Set/Reset Signals

H. Le Minh, Z. Ghassemlooy and Wai Pang Ng

Optical Communications Research Group
School of Computing, Engineering and Information Sciences
Northumbria University, Newcastle upon Tyne, NE1 8ST, UK
Email: h.le-minh@unn.ac.uk, fary.ghassemlooy@unn.ac.uk, wai-pang.ng@unn.ac.uk
Phone: +44 (0)191 227 4902, Fax: +44 (0)191 227 3684

Abstract – A novel all-optical set/reset flip-flop (AOFF) based on a symmetric Mach-Zehnder (SMZ) switch with a feedback-loop and multiple forward set/rest signals is presented. The proposed flip-flop has a fast response, a flat output gain and a short switching-on interval of a few hundreds of picoseconds regardless of the associated feedback-loop delay. It is shown that a high on/off constrast ratio at AOFF output is achieved above 20 dB.

Subject terms: All-optical flip-flop, symmetric Mach-Zehnder switch, feedback-loop

1 Introduction

All-optical flip-flop is an essential component for latching functions in high-speed all-optical processing applications [1,2]. Currently, AOFF can be realized by using the coupled/multimode-interference bi-stable laser diodes scheme [3,4] or by a SMZ with a single-pulse counter-propagation control-signal feedback-loop [5]. In the former scheme, a number of wavelengths are required, whereas in the latter scheme only a single wavelength is employed with a feedback-loop (FBL) to enhance the AOFF configuration simplicity. However, due to a real time signal-propagation delay associated with the FBL is hundreds of picoseconds [5], there is a lag in feedback

signal (i.e. requiring a sufficient transient time equivalent to the FBL delay to fully set AOFF in an ON state) when switching AOFF to the ON state. In addition, the counter-propagation between a control and input signal in SMZ will result in an additional delay in the rising and falling edges of AOFF output [6]. As the results, these proposed AOFFs operate in nanosecond order. Therefore, achieving a fast response time and an ON interval which is shorter than the transient time are the issues in feedback-loop based AOFF employing in high-speed applications. Here, we propose a new AOFF configuration assisted by a feedback-loop SMZ with multiple forward control signals (set S and reset R) to overcome these limitations.

2 AOFF Operation

An AOFF circuit block diagram and its operation principle are depicted in Fig. 1. AOFF is composed of a SMZ switch [5][7] with a continuous wave (CW) signal input, "set" and "reset" control inputs in the upper and lower control arms, respectively, and a FBL (with a signal propagation delay of T_{FBL}) feeding β% of power from AOFF output (Q) to the upper control arm of the SMZ. Polarization controllers are used to introduce an orthogonal-polarization between CW and control signals, and consequently a polarization beam splitter is used at the output of SMZ to separate them. In the absence of the optical pulses at control inputs and providing both SOAs are identical, SMZ is in a balance state due to the signal gain and phase profiles in both arms in SMZ are the same, thus CW signal propagating in both arms will not emerge at AOFF output (i.e. in OFF state). A single "set" pulse will pass through a number of paths with different delays and attenuators to produce a multiplexed pulse set S in T_{FBL}, before being applied to the upper control input of the SMZ for toggling AOFF to ON state. The first pulse of S will saturate SOA_1, thus inducing an

imbalance in gain and phase profiles between two arms and hence causing a switching CW signal to Q. For maintaining AOFF in ON state, i.e. a flat SOA gain saturation level, a portion β% of Q output power P_{FBL} is fed back to the upper control input of the SMZ. However, since P_{FBL} takes a T_{FBL} to arrive SOA_1, S pulses followed the first pulse continue maintaining the SOA_1 saturation, thus precluding gain from recovering to its initial value when the first pulse exits SOA_1 while P_{FBL} still yet arrives. Similar to the "set" pulse, a "reset" pulse, after a delay of T_{ON} (the ON interval), creates R, which is applied to the lower control input of the SMZ. The first pulse of R saturates the SOA_2 gain dropping it to the same level of SOA_1 saturating gain (i.e. restoring the gain and phase balance between SMZ arms) and once again toggling AOFF to its OFF state due to CW is no longer switched to Q. Note P_{FBL} is still in the upper control port within a subsequent T_{FBL} period although there is no output signal at Q. To retain the same gain level in both SOAs in this period, the followed pulses in R will ensure a continuous gain saturating of SOA_2 for SMZ being in balance, thus completely turning-off the Q signal during and after T_{FBL} once the "reset" signal is applied.

3 AOFF Stability

The temporal gain of the output Q is expressed by [7]:

$$Q(t) = \mathrm{K}\left[G_1(t) + G_2(t) - 2\sqrt{G_1(t)G_2(t)}\cos\left(-\frac{\alpha_{LEF}}{2}\ln\left(\frac{G_1(t)}{G_2(t)}\right)\right)\right] \quad (1)$$

where K is an overall constant coupling factor, $G_1(t)$ and $G_2(t)$ are the temporal gain profiles of SOA_1 and SOA_2. α_{LEF} is the SOA linewidth enhancement factor. It is noted that $Q(t) = 0$ when $G_1(t) = G_2(t)$. The SOA gain computed over a SOA length L_{SOA} is given by [7]:

$$G(t) = \frac{P(L_{SOA}, t)}{P(0,t)} = \exp\left(\Gamma g \int_0^{L_{SOA}} N(z,t)\Delta z \right) \tag{2}$$

where Γ is the confinement factor, g is the gain coefficient and $N(t)$ is the SOA carrier density. The gain profiles are, therefore, dependent on the temporal change of carrier which is governed by the SOA rate equation with the applied average power $P(t)$ [8]

$$\frac{\partial N(t)}{\partial t} = \frac{I_e}{qV_{SOA}} - \frac{N(t)}{\tau_e} - \frac{P(t)g[N(t) - N_T]}{h\nu A_{SOA}} \tag{3}$$

where I_e is the injection DC-current, q is the electron charge, V_{SOA} is the active volume, τ_e is the carrier lifetime, $h\nu$ is the photon energy, A_{SOA} is the cross-section area of active region and N_T is the carrier density at transparency. For achieving operation stability in AOFF, the feedback power is constrained to match with the average powers of both S and R signals. This will ensure the steady imbalance and balance states in SMZ during the transient durations when AOFF is switched to ON and OFF states, respectively. These constraints are represented as follows:

$$P_{FBL} = \sum_{m=0}^{M-1} P_{S.avg}\left(t + \frac{mT_{Loop}}{M} \right) \tag{4}$$

$$\sum_{m=0}^{M-1} P_{R,avg}\left(t + \frac{mT_{Loop}}{M} \right) = \frac{P_{FBL}}{2} \tag{5}$$

where $P_{S,avg}(t)$ and $P_{R,avg}(t)$ are the average powers of control pulses in S and P streams, respectively, over T_{FBL}. M is the number of pulses in each S or R. In (4), if P_{FBL} is smaller than the average power of the applied control signal S, Q signal will eventually be ceased. However, a greater P_{FBL} will gradually saturate SOA gain, thus saturating AOFF-output gain. As those results, Q is varied in a large intensity range, which is determined by the intensity variation ratio (IVR) between the minimum and

the maximum values of Q signal during T_{ON}. For a complete turning-off in AOFF, the applied average power of control signal R is required to be half of P_{FBL} ensuring both SOAs being received a same average control power. In case this power is different from P_{FBL}, a residual signal will emerge at the output Q which in turn unexpectedly restores AOFF to the ON state again. This residual signal will therefore deteriorate the on/off contrast ratio (CR) at Q, which is defined by the power ratio of signals in ON and OFF states.

4 Results and Discussions

The AOFF operation is validated using the VPI simulation software. Simulation and SOA device parameters are given in Table 1. Note that the average power of S is greater 3 dB compared to R due to S is reduced by 3 dB when being coupled with P_{FBL} to ensure that SOAs are excited with same set/reset powers. T_{FBL} is approximated of 0.2 ns equivalent to a 40-mm optical waveguide FBL [5]. SOA model is assumed to be polarization-independent, though in practical systems, polarization-gain-dependence (~1 to 2 dB) and the imperfect polarization states of CW and S/R signals will slightly affect on AOFF operation. The flip-flop operation is illustrated in Fig. 2. Series of “set” and “reset” single pulses, shown in Fig. 2(a), are applied to the AOFF in a range of T_{ON} values of 0.1, 0.2, 0.5, 1, 2 and 5 ns. The resultant temporal gain profiles of SOAs corresponding with set/reset signals are observed in Fig. 2(b). During a period of T_{ON}, SOA_1 gain is kept at the same saturation level by both of S and P_{FBL}. Figure 2(c) displays the AOFF output waveforms. There are ripples at the leading edge of Q output signal in ON state during a T_{FBL} owing to the variation in the SOA_1 gain profile caused by the discrete excitations on SOA_1 by pulses in S. When AOFF is switched off, a small residual

signal, lasting in T_{FBL}, still emerges at Q. This is due to the gain variation of SOA_2 caused by multiple–pulse excitations of R in contrast to a flat gain profile of SOA_1 maintained by a left-over of constant P_{FBL} within that T_{FBL}, hence, causing ripples at the trailing edge of Q signal. It will, therefore, result in on/off CR deterioration.

The graphs in Fig. 3 show that the highest achieved CR is 22 dB at β = 15% (AOFF total output power is 14.5 dB, see Fig. 2(c)) where the conditions in (4) and (5) are satisfied, at T_{ON} = 1ns. It is also shown that the AOFF output signal is relatively flat during T_{ON} with the observed IVR is 0.95. Beyond this optimum operation point, both CR and IVR are considerably decreased due to high residual power and improper feedback power, respectively. Note that high β results in flat-level performance in CR and IVR, however, since SOA_1 gain is saturated due to high-power P_{FBL}, their values are noticeably small.

5 Conclusions

A new AOFF configuration based on a SMZ with FBL and multiple-pulse forward set/reset signals was proposed. Multiple-set/rest control-signal scheme fully overcome the feedback-loop delay, thus making AOFF suitable for high-speed memory or signal processing applications where T_{ON} is required as small as a few hundred of picoseconds regardless of FBL delay. In addition, the forward controls enhanced the AOFF toggling response within pulse width of set and reset signals. On/off contrast and intensity variation ratios are achieved of 22 dB and 0.95, respectively, at the optimum operating point.

References

1 F. Ramos, E. Kehayas, J. M. Martinez, R. Clavero, J. Marti, L. Stampoulidis, D. Tsiokos, H. Avramopoulos, J. Zhang, P. V. Holm-Niesen, N. Chi, P. Jeppersen, N. Caenegem, D. Colle, M. Pickavet, and B. R. Ti, “IST-LASAGNE: Towards all-optical label swapping employing optical logic gates and optical flip-flops”, IEEE Light. Tech., vol. 23, pp. 2993-3011, 2005

2 M. T. Hill, A. Srivatsa, N. Calabretta, Y. Liu, H. d. Waardt, G. D. Khoe, and H. J. S. Doren, “1x2 optical packet switch using all-optical header processing”, Electron. Lett., vol. 37, pp. 774-775, 2001

3 M. T. Hill, H. d. Waardt, G. D. Khoe, and H. J. S. Doren, “All-optical flip-flop based on coupled laser diodes”, IEEE Quan. Electron., vol. 37, pp. 405-413, 2001

4 M. Takenaka, M. Raburn, and Y. Nakano, “All-optical flip-flop multimode interference bistable laser diode”, IEEE Photon. Tech. Lett., vol. 17, pp. 968-970, 2005

5 R. Clavero, F. Ramos, J. M. Martinez, and J. Marti, “All-optical flip-flop based on a single SOA-MZI”, IEEE Photon. Tech. Lett., vol. 17, pp. 843-845, 2005

6 B. C. Wang, V. Baby, W. Tong, L. Xu, M. Friedman, R. J. Runster, I. Glesk, and P. Prucnal, “A novel fast optical switch based on two cascaded Terahertz Optical Asymmetric Demultiplexers (TOAD)”, Opt. Express, vol. 10, pp. 15-23, 2002

7 Z. Ghassemlooy and R. Ngah, "Simulation of 1x2 OTDM router employing symmetric Mach-Zehnder switches," IEE Proc. Circ. Devi. Syst., vol. 152, pp. 171-177, 2005

8 G. P. Agrawal and N. A. Olsson, "Self-Phase Modulation and spectral broadening of optical pulses in semiconductor laser amplifiers," IEEE Quan. Elec., vol. 25, pp. 2297-2306, 1989

Table and Figure captions:

Table 1: Simulation and SOA device parameters

Figure 1: Multi-forward-control AOFF configuration

Figure 2: (a) Set/Reset pulses, (b) temporal gain profiles of SOA_1 and SOA_2 and (c) AOFF output (Q)

Figure 3: AOFF IVR and CR against β (at T_{ON} = 1ns)

Table 1: Simulation and SOA device parameters

Parameters	Value
Input power P_{CW}	0 dBm
Gaussian pulse width	20 ps
Signal wavelength	1554 nm
P_S (peak power of first pulse)	13.5 dBm
P_S (peak power of followed pulses)	8.5 dBm
P_R (peak power of first pulse)	10.5 dBm
P_R (peak power of followed pulses)	5.5 dBm
SOA linewidth enhancement factor α_{LEF}	5
SOA length L_{SOA}	0.5 mm
SOA confinement factor Γ	0.2
SOA carrier density at transparency N_T	1.4×10^{24} m^{-3}
SOA spontaneous emission factor n_{sp}	2
DC-bias I_e	150 mA
FBL delay T_{FBL}	0.2 ns
Splitting factor β	15%

Figure 1: Multi-forward-control AOFF configuration

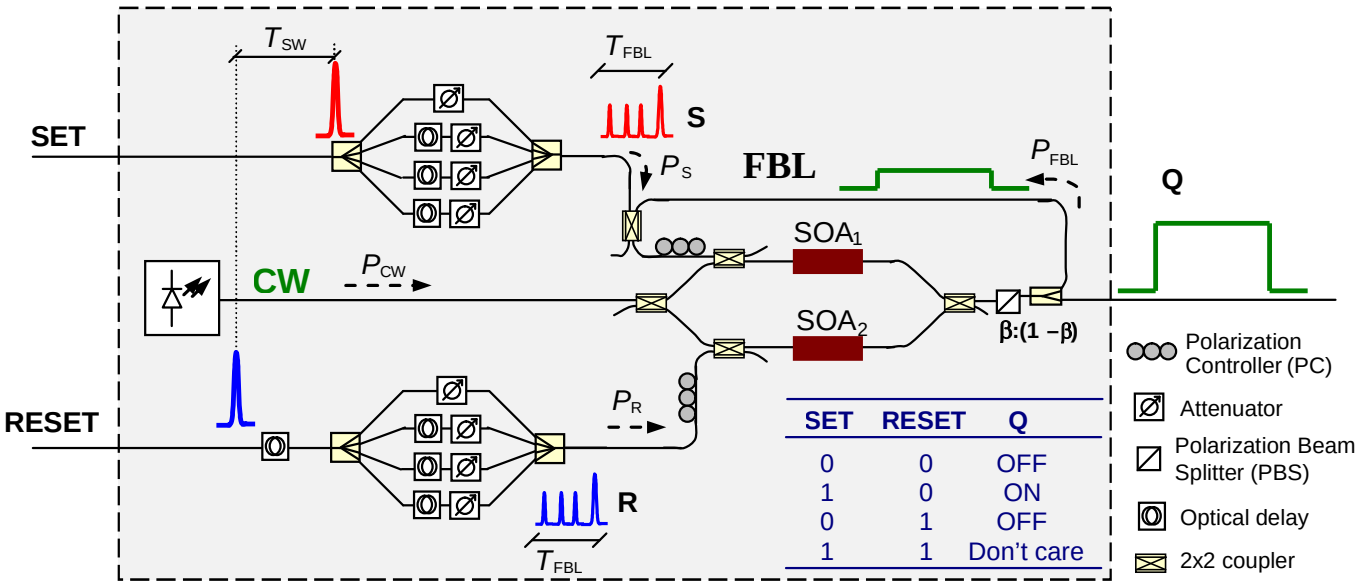

Figure 2: (a) Set/Reset pulses, (b) temporal gain profiles of SOA_1 and SOA_2 and (c) AOFF output (Q)

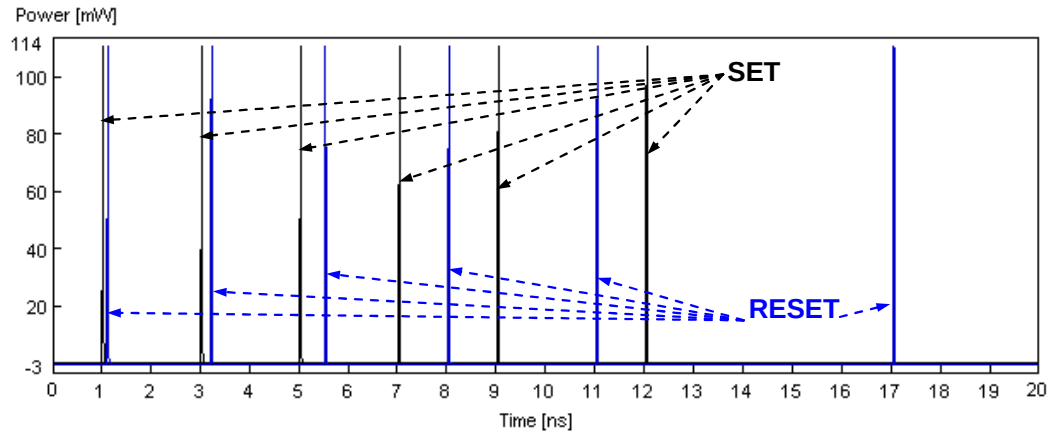

(a)

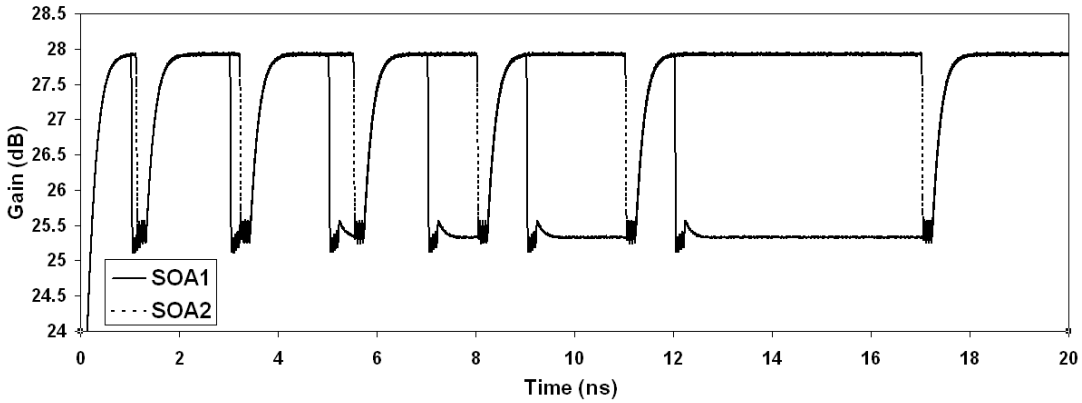

(b)

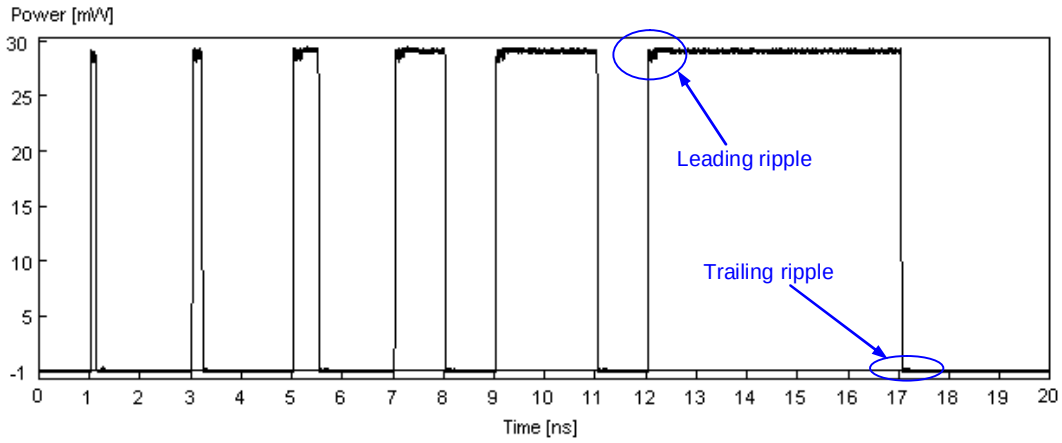

(c)

Figure 3: AOFF IVR and CR against β (at T_{ON} = 1ns)